JOURNAL OF COMPUTATIONAL PHYSICS 118, 180–188 (1995)

Electrostatic Field in Inhomogeneous Dielectric Media II. Volume Element Method

NARENDRA S. GOEL, ZHONGLIN KO, AND FENGSHI GANG

Department of Computer Science, Wayne State University, Detroit, Michigan 48202

Received July 26, 1994

A novel computationally fast approach, the volume element method, for calculating the electrostatic field in arbitrary inhomogeneous dielectric media with open boundary condition is presented. The method is tested for accuracy by comparing the numerically calculated electrostatic fields against those analytically obtained for a dielectric sphere and a dielectric ellipsoid in a uniform field and a dielectric sphere near a charge.

1. INTRODUCTION

In the first paper in this series [1] we summarized different numerical methods for calculating electrostatic potential and field for an arbitrary-shaped inhomogeneous dielectric medium with open boundary condition. We presented a novel, computationally fast, and general approach for solving such problems. This approach consisted of two main steps. In step 1, one tessellates the space of interest into cubical cells and calculates the effective dielectric constants for each cell using a so-called effective parameter for interfacial cells (EPIC) method. In step 2, one solves the electrostatic problem by placing an appropriate charge distribution on the boundaries of cells.

In this paper, we describe another method in which one still follows step 1, but in step 2 one solves the electrostatic problem by placing appropriate fictitious charges *inside* each cell. We refer to this method as the volume element method (VEM). Step 1 is described in detail in the first paper and here we assume that we have a space consisting of cubical cells, each cell in general consisting of materials of different dielectric properties.

The next section is devoted to the description and details of the volume element method. As in the first paper, we evaluate this method by comparing the results obtained by this method against analytical results from three cases of (1) a dielectric sphere in a uniform electric field; (2) a dielectric ellipsoid in a uniform electric field, and (3) a dielectric sphere in a point charge field. This evaluation of the method is given in Section 3. As we will see, the volume element method is somewhat less accurate than the indirect boundary element method of the first paper but is computationally faster. In Section 4, we make a few concluding remarks and point out directions for future research.

2. VOLUME ELEMENT METHOD

As noted in the Introduction, we use the EPIC method, described in the first paper in this series [1], to replace the problem of an arbitrary shaped dielectric inhomogeneous medium with $N \times N \times N$ cubic cells, each consisting of only one kind of material, with effective dielectric parameters specified for each cell.

In general, due to changes in the dielectric constant, we would have a polarized surface charge on the boundary between the cells as well as a volume charge inside the cell. In the volume element method, we assume that the polarized charge is only inside the cell volume and the impending field is the sum of fields due to these charges. The surface charges on the boundaries between cells is minimized by volume linearization of effective dielectric parameters so that there is no abrupt change of dielectric parameters between two neighboring cells. This volume linearization is described in the next subsection, which is followed by the general formulation of the approach and specific details.

2.1. *Volume Linearization*

Consider three neighboring volume elements $i-1$, i, and $i+1$ (see Fig. 1a), with effective dielectric constants ε^{i-1}, ε^{i}, and ε^{i+1}, respectively, as calculated by using EPIC. Let us for the moment focus on the x-direction. Our goal is to find another set of dielectric constants for each cell, such that there is minimal discontinuity of dielectric constants between neighboring cells. Intuitively, for the interface between two cells one can take either the arithmetic average (see Fig. 1b) or the harmonic average (see Fig. 1c) of two neighboring cells, or a simple average of these two averages; i.e., for the interface between $i-1$ and i cells,

$$\varepsilon_x^{i-1,i} = \left(\frac{2\varepsilon_x^{i-1}\varepsilon_x^{i}}{\varepsilon_x^{i-1}+\varepsilon_x^{i}} + \frac{\varepsilon_x^{i-1}+\varepsilon_x^{i}}{2} \right) \Big/ 2, \tag{1}$$

with a similar formula for $\varepsilon_x^{i,i+1}$ for the interface between i and $i+1$ cells. To ensure continuity of the dielectric constant, we then assume for the dielectric constant of cell i the average value

0021-9991/95 $6.00

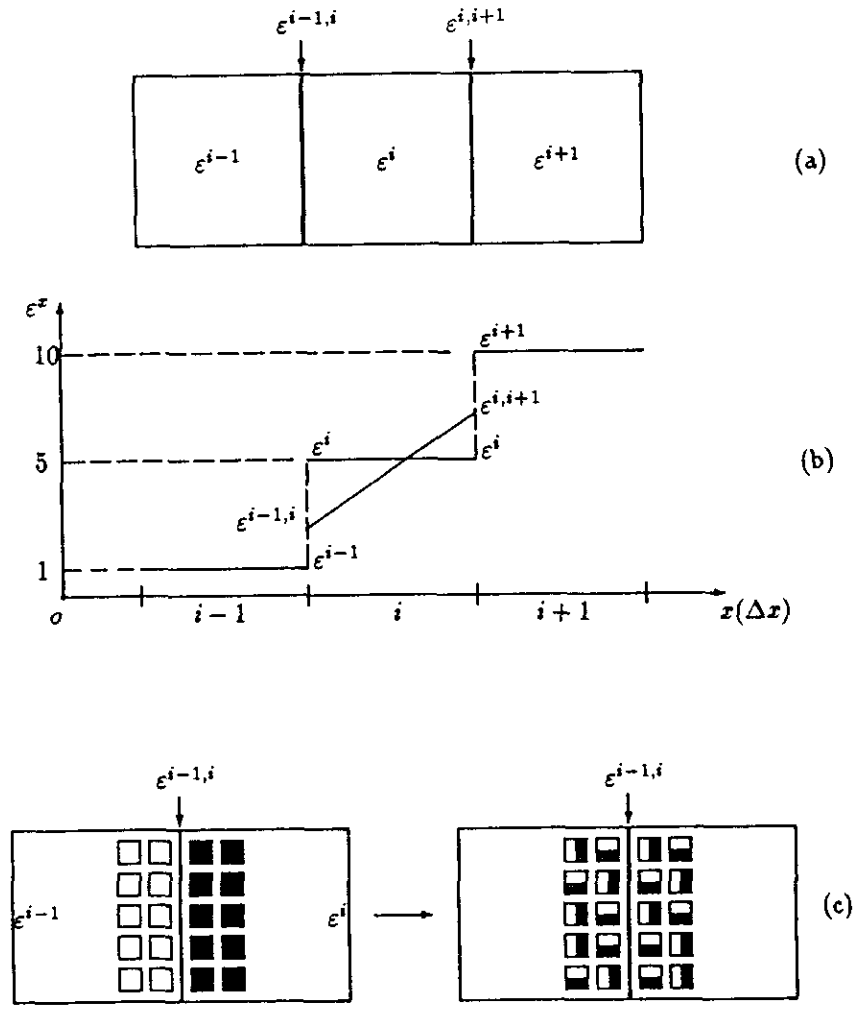

FIG. 1. Volume linearization.

$$\overline{\varepsilon_x^i} = \frac{\varepsilon_x^{i-1,i} + \varepsilon_x^{i,i+1}}{2} \tag{2}$$

and for the gradient of the dielectric constant in cell i the value

$$\overline{\frac{\partial \varepsilon_x^i}{\partial x}} = \frac{\varepsilon_x^{i,i+1} - \varepsilon_x^{i-1,i}}{\Delta x}, \tag{3}$$

where Δx is the width of the cell i in the x-direction. We carry out similar calculations for the y and z directions.

The average dielectric constant and its gradient, as given by Eqs. (2) and (3), will be the parameters which we use in the rest of this paper. For simplicity, we drop the bar and let $(\varepsilon_x, \varepsilon_y, \varepsilon_z)$ and their derivatives represent the average values for the volume elements and not the effective parameters used by EPIC.

We should note that there are many ways to specify the interfacial dielectric constant. We tried the arithmetic average, the harmonic average, and the simple average of these averages [Eq. (1)] and found the last one to be the most accurate in terms of calculation of electrostatic fields.

2.2. *Formulation*

The electrostatic potential Φ on an arbitrary point (x, y, z) in a homogeneous dielectric medium of dielectric constant $(\varepsilon_x, \varepsilon_y, \varepsilon_z)$ in the presence of a free charge density ρ_0 is given by the Maxwell equation

$$\varepsilon_x \frac{\partial^2 \Phi}{\partial x^2} + \varepsilon_y \frac{\partial^2 \Phi}{\partial y^2} + \varepsilon_z \frac{\partial^2 \Phi}{\partial z^2} + \frac{\partial \varepsilon_x}{\partial x}\frac{\partial \Phi}{\partial x} + \frac{\partial \varepsilon_y}{\partial y}\frac{\partial \Phi}{\partial y} + \frac{\partial \varepsilon_z}{\partial z}\frac{\partial \Phi}{\partial z} = -\frac{1}{\varepsilon_0}\rho_0, \tag{4}$$

where ε_0 is the dielectric constant of the free space.

The potential Φ can be decomposed into two parts: the initial

polarized field Φ_0 due to ρ_0 and the impending field Φ_ρ caused by polarization of dielectrics:

$$\Phi = \Phi_0 + \Phi_\rho. \tag{5}$$

Substituting Eq. (5) into Eq. (4), we get

$$\begin{aligned}\varepsilon_x \frac{\partial^2 \Phi_\rho}{\partial x^2} + \varepsilon_y \frac{\partial^2 \Phi_\rho}{\partial y^2} + \varepsilon_z \frac{\partial^2 \Phi_\rho}{\partial z^2} + \frac{\partial \varepsilon_x}{\partial x}\frac{\partial \Phi_\rho}{\partial x} \\ + \frac{\partial \varepsilon_y}{\partial y}\frac{\partial \Phi_\rho}{\partial y} + \frac{\partial \varepsilon_z}{\partial z}\frac{\partial \Phi_\rho}{\partial z} = -\frac{1}{\varepsilon_0}\rho_0 - \\ \left\{\varepsilon_x \frac{\partial^2 \Phi_0}{\partial x^2} + \varepsilon_y \frac{\partial^2 \Phi_0}{\partial y^2} + \varepsilon_z \frac{\partial^2 \Phi_0}{\partial z^2}\right. \\ \left. + \frac{\partial \varepsilon_x}{\partial x}\frac{\partial \Phi_0}{\partial x} + \frac{\partial \varepsilon_y}{\partial y}\frac{\partial \Phi_0}{\partial y} + \frac{\partial \varepsilon_z}{\partial z}\frac{\partial \Phi_0}{\partial z}\right\}.\end{aligned} \tag{6}$$

Here Φ_0, Φ_ρ should satisfy the following equations

$$\nabla \Phi_0 = -\frac{1}{\varepsilon_0}\rho_0 \tag{7}$$

and

$$\nabla \Phi_\rho = -\frac{1}{\varepsilon_0}\rho, \tag{8}$$

where ρ_0 is the polarized charge volume density.

As noted earlier in the volume element method, we assume that each cell has a volume polarized charge density and that the impending field is caused by all these volume charges. Specifically, we number all the $n = N \times N \times N$ volume elements (cubical cells) from 1 to n. For each element j ($1 \le j \le n$) we assume a polarized charge volume density ρ_j. Let us denote the field caused by this volume charge as Φ_ρ^j. Thus

$$\Phi\rho = \sum_{j=1}^{n} \Phi_\rho^j. \tag{9}$$

Let us denote the right hand of Eq. (6) for a volume element i by $-\rho_p^i$ (where ρ_p^i could be called a pseudo charge density):

$$\begin{aligned}\rho_p^i = \frac{1}{\varepsilon_0}\rho_0^i + \varepsilon_x^i \frac{\partial^2 \Phi_0^i}{\partial x^2} + \varepsilon_y^i \frac{\partial^2 \Phi_0^i}{\partial y^2} + \varepsilon_z^i \frac{\partial^2 \Phi_0^i}{\partial z^2} \\ + \frac{\partial \varepsilon_x^i}{\partial x}\frac{\partial \Phi_0^i}{\partial x} + \frac{\partial \varepsilon_y^i}{\partial y}\frac{\partial \Phi_0^i}{\partial y} + \frac{\partial \varepsilon_z^i}{\partial z}\frac{\partial \Phi_0^i}{\partial z}.\end{aligned} \tag{10}$$

Substituting Eq. (9) into Eq. (6) and using Eq. (10), we get for each volume element i ($1 \le i \le n$)

$$\begin{aligned}\sum_{j=1}^{n}\left(\varepsilon_x^i \frac{\partial^2 \Phi_\rho^{i,j}}{\partial x^2} + \varepsilon_y^i \frac{\partial^2 \Phi_\rho^{i,j}}{\partial y^2} + \varepsilon_z^i \frac{\partial^2 \Phi_\rho^{i,j}}{\partial z^2}\right. \\ \left. + \frac{\partial \varepsilon_x^i}{\partial x}\frac{\partial \Phi_\rho^{i,j}}{\partial x} + \frac{\partial \varepsilon_y^i}{\partial y}\frac{\partial \Phi_\rho^{i,j}}{\partial y} + \frac{\partial \varepsilon_z^i}{\partial z}\frac{\partial \Phi_\rho^{i,j}}{\partial z}\right) = -\rho_p^i,\end{aligned} \tag{11}$$

where $\Phi_\rho^{i,j}$ is the potential field at volume i caused by polarized charge density in volume j.

If we denote the polarized field caused at volume element i due to a unit polarized charge in volume element j by $\Psi_\rho^{i,j}$, then

$$\Phi_\rho^{i,j} = \rho^j \Psi_\rho^{i,j} \tag{12}$$

and Eq. (11) can be written as

$$\sum_{j=1}^{n} a_{i,j}\rho^j = -\rho_p^i \qquad (1 \le i \le n), \tag{13}$$

where

$$\begin{aligned}a_{i,j} = \varepsilon_x^i \frac{\partial^2 \Psi_\rho^{i,j}}{\partial x^2} + \varepsilon_y^i \frac{\partial^2 \Psi_\rho^{i,j}}{\partial y^2} + \varepsilon_z^i \frac{\partial^2 \Psi_\rho^{i,j}}{\partial z^2} \\ + \frac{\partial \varepsilon_x^i}{\partial x}\frac{\partial \Psi_\rho^{i,j}}{\partial x} + \frac{\partial \varepsilon_y^i}{\partial y}\frac{\partial \Psi_\rho^{i,j}}{\partial y} + \frac{\partial \varepsilon_z^i}{\partial z}\frac{\partial \Psi_\rho^{i,j}}{\partial z}.\end{aligned} \tag{14}$$

The basic idea behind the volume element method is to calculate polarized charge densities ρ^j in volume element j($1 \le j \le n$) by solving the matrix equation Eq. (13) and then to calculate the impending field by summing the fields caused by these charge densities. However, to do this one needs to calculate pseudo charge densities ρ_p^j and the matrix elements $a_{i,j}$. These charge densities can be calculated by using Eq. (10) and the average dielectric constants and their gradients as given by Eqs. (2) and (3). The calculation of matrix elements $a_{i,j}$ is described in the next subsection.

2.3. *Matrix Evaluation*

From Eq. (14), $a_{i,j}$ is determined by the dielectric constant ($\varepsilon_x^i, \varepsilon_y^i, \varepsilon_z^i$) and its spatial derivatives, given by Eqs. (2) and (3), and by $\Psi_\rho^{i,j}$ whose calculation is described below.

Consider a uniformly distributed charge in volume element j of unit volume density. Let the center of this volume element be the origin of the coordinate system. Let $\vec{r_{i,j}}$ denote the vector from the center of volume j to the center of volume i. Let $d_{i,j}$ denote the length of this vector and ($r_{i,j}^x, r_{i,j}^y, r_{i,j}^z$) its x, y, and z components.

For large $d_{i,j}$, the volume charge in element j can be treated as a point charge at its center and the potential due to element

j at the center of element i can be taken to be the same at all points inside the element i. For this case [2],

$$\frac{\partial^2 \Psi_\rho^{i,j}}{\partial x^2} = -\frac{q}{4\pi\varepsilon_0}\left(\frac{1}{d_{i,j}^3} - \frac{3(r_{i,j}^x)^2}{d_{i,j}^5}\right), \tag{15}$$

where q is the total charge in element j (which in this case is the volume of the element j, the volume charge density being equal to 1), with similar equations for the y and z directions.

For small $d_{i,j}$, when volume element i is close to element j, theoretically it should be better to subdivide each of the volume elements i and j further, calculate the gradient of the potential field for each pair of subvolumes, and then average them to get a better estimate of $\Psi_\rho^{i,j}$. However, our calculation shows that there is no real difference in the results with and without subdivisons. Therefore, we use Eq. (15) for all pairs of volume elements i and j ($i \neq j$).

When $i = j$, $d_{i,j} = 0$, one needs to calculate only the self-induced field $\Psi_\rho^{i,i}$ which is the field of uniformly distributed charge in volume element i of unit volume charge density. Therefore, it satisfies the equation

$$\frac{\partial^2 \Psi_\rho^{i,i}}{\partial x^2} + \frac{\partial^2 \Psi_\rho^{i,i}}{\partial y^2} + \frac{\partial^2 \Psi_\rho^{i,i}}{\partial z^2} = -\frac{1}{\varepsilon_0}. \tag{16}$$

Because of the symmetric distribution of charge in volume i,

$$\frac{\partial^2 \Psi_\rho^{i,i}}{\partial x^2} = \frac{\partial^2 \Psi_\rho^{i,i}}{\partial y^2} = \frac{\partial^2 \Psi_\rho^{i,i}}{\partial z^2} = -\frac{1}{3\varepsilon_0}. \tag{17}$$

Integrating Eq. (17), one obtains

$$\frac{\partial \Psi_\rho^{i,i}}{\partial x} = -\frac{x}{3\varepsilon_0}. \tag{18}$$

Averaging this gradient for all values of x within element i gives a value zero for the whole volume element, i.e.,

$$\frac{\partial \psi_\rho^{i,i}}{\partial x} = 0. \tag{19}$$

Combining Eq. (17) with Eq. (4) one obtains

$$a_{i,i} = \frac{\varepsilon_x^i + \varepsilon_y^i + \varepsilon_z^i}{3\varepsilon_0}. \tag{20}$$

Now that we have all the matrix elements $a_{i,j}$ evaluated, we are ready to solve Eq. (13) for the polarized charge in each of the volume elements. However, before we do so, we need to discuss an important point, namely the elimination of the non-boundary volume elements, which will greatly reduce the size of the matrix $a_{i,j}$.

2.4. *Elimination of Non-Boundary Volume Elements*

The matrix size is determined by the total number n of volume elements. But there is a simple way to reduce the total volume with which we need to be concerned. Physically, the polarization charge occurs only between the boundaries of two volume elements with different dielectric constants. However, the EPIC approach [1], followed by volume linearization (Section 2.1) causes the boundary surface to disappear. Therefore, instead we use the concepts of boundary volume element and non-boundary volume element.

We define the non-boundary volume element as the volume element which satisfies the properties.

$$\varepsilon_x = \varepsilon_y = \varepsilon_z = \varepsilon \tag{21a}$$

and

$$\frac{\partial \varepsilon_x}{\partial x} = \frac{\partial \varepsilon_y}{\partial y} = \frac{\partial \varepsilon_z}{\partial z} = 0. \tag{21b}$$

In other words, non-boundary elements have an isotropic dielectric constant which remains constant over the entire volume. We will now show that for such volume elements the polarized charge density can be calculated easily and that this density is zero if there is no free charge in this volume.

For such a volume, for Eqs. (21) and (10), the pseudo-charge density is given by

$$-\rho_p^i = -\frac{1}{\varepsilon_0}\rho_0 - \varepsilon^i\left(\frac{\partial^2 \Phi_0^i}{\partial x^2} + \frac{\partial^2 \Phi_0^i}{\partial y^2} + \frac{\partial^2 \Phi_0^i}{\partial z^2}\right). \tag{22}$$

Since the initial field in this volume must satisfy the Poisson equation

$$\frac{\partial^2 \Phi_0^i}{\partial x^2} + \frac{\partial^2 \Phi_0^i}{\partial y^2} + \frac{\partial^2 \Phi_0^i}{\partial z^2} = -\frac{1}{\varepsilon_0}\rho_0^i.$$

Equation (22) becomes

$$-\rho_p^i = -\frac{1-\varepsilon^i}{\varepsilon_0}\rho_0^i. \tag{23}$$

For such elements, from Eq. (14),

$$a_{i,j} = \varepsilon^i\left(\frac{\partial^2 \Psi_\rho^{i,j}}{\partial x^2} + \frac{\partial^2 \Psi_\rho^{i,j}}{\partial y^2} + \frac{\partial^2 \Psi_\rho^{i,j}}{\partial z^2}\right) \qquad (i \neq j)$$

which by using Eq. (15) simplifies to

$$a_{i,j} = -\varepsilon^i \frac{q}{4\pi\varepsilon_0}\left(\frac{3}{d_{i,j}^3} - \frac{3d_{i,j}^2}{d_{i,j}^5}\right)$$
$$= 0 \qquad (i \neq j) \tag{24}$$

This equation implies that there are no dielectric effects caused on non-boundary elements by other volume elements.

From Eq. (20), the self-caused effect is given by

$$a_{i,i} = -\frac{\varepsilon^i}{\varepsilon_0}. \tag{25}$$

Substituting Eqs. (23) and (25) into the basic matrix equation (13), we obtain

$$-\frac{\varepsilon^i}{\varepsilon_0}\rho^i = -\frac{1-\varepsilon^i}{\varepsilon_0}\rho_0^i$$

or

$$\rho^i = \frac{1-\varepsilon^i}{\varepsilon^i}\rho_0^i. \tag{26}$$

Thus, for non-boundary volume elements, the polarized charge density is determined only by the initial free charge density and the dielectric constant of the volume element. If the free charge density is zero, the polarized charge density is also zero.

This discussion clearly shows that one should take out the non-boundary volume element right from the beginning from the matrix equation (13) and thus reduce the matrix size. For the case of a dielectric sphere in vacuum, when the whole space is divided into $14 \times 14 \times 14 = 1744$ volume elements, the removal of non-boundary volume elements (which are boundary elements) drops the number to 928, dropping the matrix size $a_{i,j}$ from 1744×1744 to 928×928. We denote by B the total number of boundary volume elements.

2.5. *Solving Matrix Equation and Calculation of Impending Field*

The matrix in Eq. (13) is in general a dense and asymmetric matrix but it has the property of diagonal elements being dominant. Therefore, we can use the standard Gauss–Seidel method to solve Eq. (13). (We note that the over-relaxation version of this method causes convergence to slow down, therefore we use the standard version only.)

The solution of the matrix equation (13) gives the polarized charge densities in each volume element. One can then use any discrete method to calculate the impending field at an arbitrary point. By adding the initial field to this field [Eq. (5)], one then obtains the total final potential field. One can also easily calculate the total induced charge and various moments of charges (e.g., dipole moment).

3. IMPLEMENTATION, EXPERIMENTS, AND RESULTS

To recap, the volume element method described above consists of the following steps:

1. Take as input the geometrical shapes of different dielectric objects together with their dielectric properties.
2. Divide the space into a cubical grid and run the computer-graphics-based algorithmic version of EPIC [1] to get the effective dielectric constants for each of the cubical cells.
3. Carry out the volume linearization to calculate average dielectric constants and their gradients, to minimize surface charges at boundaries between volume elements.
4. Use the initial field and initial free charge density to calculate pseudo charge densities in each volume element.
5. Determine the non-boundary volume elements and calculate the polarized charge for these elements.
6. Evaluate the matrix element $a_{i,j}$ for all pairs of boundary volume elements.
7. Solve the matrix equation to calculate polarized volume charge densities in each of the volume elements.
8. Calculate the impending field and the total field and any other global information like total charge on dipole moment.

We have written a computer program in C language and have implemented the method on SUN SPARCstation 10. We tested our method against analytical results for the same three cases discussed in [1] presented below. Before we give the results, let us make a few general observations.

a. A conducting material is approximated by a dielectric material of dielectric $\varepsilon = 10^5$.

b. As could be expected, the computer time depends upon the number of cells into which the space is divided. For the resolution level of $5 \times 5 \times 5$ cells, the computer time is about 5 sec. This time increases to about 20 sec for resolution of $10 \times 10 \times 10$ and to about 20 min for resolution of $20 \times 20 \times 20$. This non-linear increase is expected, since as the resolution is doubled, the number of volume elements is increased by a factor of 8 and the number of matrix elements (without deleting those elements associated with non-boundary volume elements) by a factor of $8^2 = 64$. A lower level resolution is desired from a computational efficiency point of view but a higher level resolution is warranted for accurate estimation of electrostatic fields inside the dielectrics (where there is no real non-boundary volume element). We found a good balance between efficiency and accuracy for a resolution level of $10 \times 10 \times 10$. In the following we give results for this resolution level.

3.1. *Dielectric Sphere in a Uniform Field*

Here we have a dielectric sphere of radius 0.5, embedded in a uniform electric field of strength 100, parallel to the z-direction. In Table I is given the comparison between numerical

TABLE I

Comparison of Numerically Calculated and Analytical Results for the Dipole Moment (in the z-Direction) and Total Positive Charge for a Dielectric Sphere in a Uniform Electric Field of Strength 100 in the z-Direction

Dielectric constant ε	Dipole moment			Total positive charge		
	Calculated	Analytical	% Difference	Calculated	Analytical	% Difference
5	89.31	89.76	−0.50	132.92	134.64	−1.28
25	141.41	139.63	1.27	207.73	209.44	−0.82
10^5	165.21	157.08	5.17	239.11	235.61	1.49

analytic results for a dipole moment in the z-direction (dipole moments on the x and y directions are zero for both numerical and analytical cases) and the total positive charge. We can see that for the dielectric sphere the calculation of the dipole moment is quite accurate and this accuracy decreases to about 5% as the sphere becomes a conducting sphere. The numerical method slightly underestimates the total charge for the dielectric sphere and overestimates it for the conducting sphere.

A better comparison between numerically calculated and analytical results is presented in Figs. 2a and 2b where we plot the total electrostatic field in the x–y plane for $z = 0$ for a dielectric sphere. By comparing these figures, we note that in general the numerically calculated field agrees well with the analytical results for both inside and outside the dielectric sphere. The slight difference is near the boundary of sphere: for the analytic approach, there is a jump in the field while this field changes smoothly for the numerical case, because volume linearization methods smooth away the discontinuities between different dielectric media. It should be noted that the field inside the sphere is lower than the external field and higher outside the sphere due to polarized charges.

To summarize, our numerical method gives results for electrical quantities of interest (field, total charge, dipole moment) to within 2% for a large range of dielectric constants ($\varepsilon \leq 1000$) and to within about 5% for near-conducting sphere.

3.2. *Dielectric Ellipsoid in a Uniform Field*

We choose an ellipsoid with semi-axes of 3, 4, and 5, i.e., the one whose surface is defined by the equation

$$\frac{x^2}{3^2} + \frac{y^2}{4^2} + \frac{z^2}{5^2} = 1. \tag{27}$$

We take an initial field parallel to the z-axis, with a strength of 10.

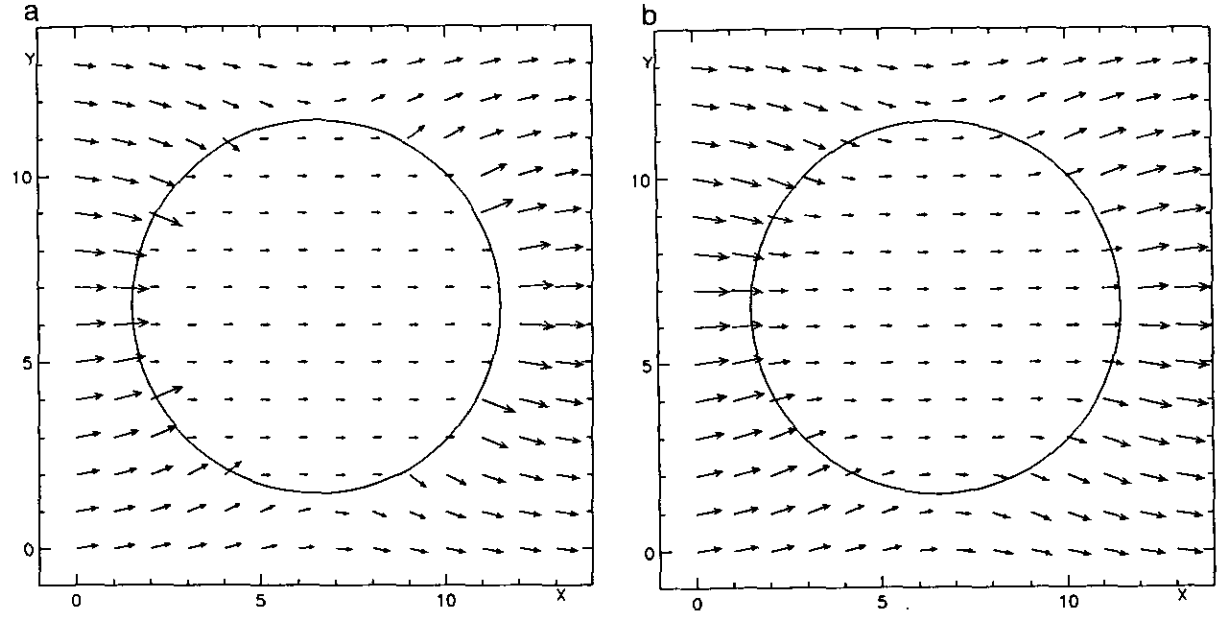

FIG. 2. (a) Analytically calculated E field in the x–y plane at $z = 0$ for $\varepsilon = 5$. (b) Same as (a) except for a numerically calculated field.

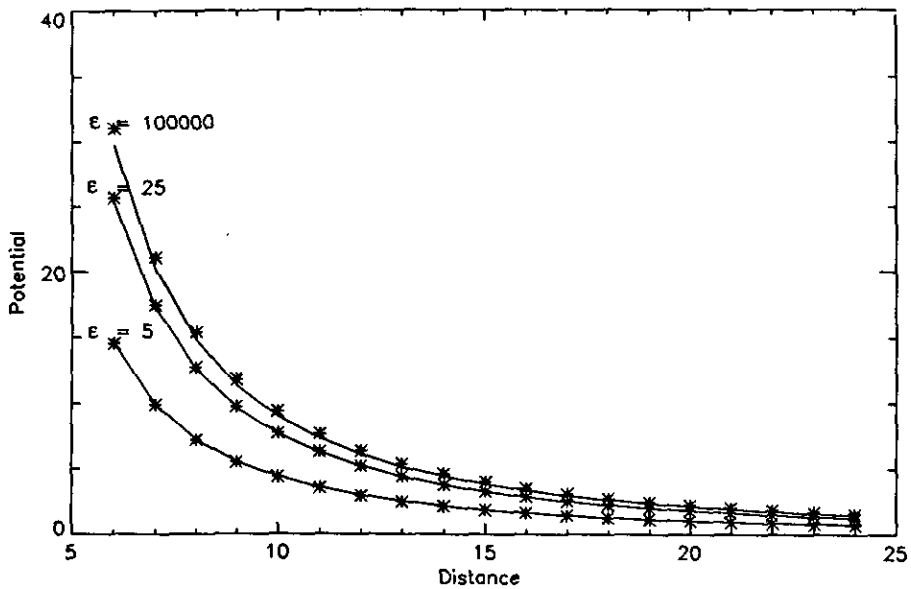

FIG. 3. Impending potential outside the ellipsoid of dielectric constants $\varepsilon = 5$, 25, and 10^5. Solid line represents analytical results while * denotes numerically calculated values.

In Table II we give the comparison between numerically calculated and analytical results for the dipole moment and impending electric field inside the ellipsoid, both in the z-direction (we omit the comparison for the total positive charge as we did for the case of the sphere because the value for the analytical case is not available). The impending potential outside the ellipsoid is plotted in Fig. 3 for both numerical and analytical methods.

Table II and Fig. 3 show that the numerical method gives results within 2% for a dielectric ellipsoid and within 5% for a near conducting ellipsoid.

3.3. *Dielectric Sphere in a Point Charge Field*

This case is similar to the first case expect that the initial field is caused by a point charge of value 2000 located at a distance d ($d > 0.5$) from the center of the sphere along the z-axis.

In Table III are given the dipole moments along the z-direction for $d = 3$ as calculated numerically and analytically. One can see that for this case the accuracy of the numerical method is comparable to that for a sphere in a parallel field.

But when the point charge is brought close to the sphere, the numerical method has a problem. One of the physical constraints is that the total positive polarized (TPP) charge should equal the total negative polarized (TNP) charge. Let us call this constraint a zero total charge constraint. For the present case, this constraint is not satisfied well. For example, for $d = 1.0$ the TPP = 220.4 and TNP = −204.2 (% difference = 7.34), while for $d = 0.7$ the TPP = 505.5 and TNP = −421.9 (% difference = 16.54). This violation of the physical constraint could be caused either by EPIC or volume linearization. To investigate these possibilities, we made the grid finer in EPIC, but the constraint was still violated. In volume linearization, using the arithmetic average value for the interfacial cell dielec-

TABLE II

Comparison of Numerically Calculated and Analytical Results for the Dipole Moment (in the z-Direction) and Impending Field in the z-Direction Inside a Dielectric Ellipsoid of Semi-axes 3, 4, and 5, Kept in a Uniform Electric Field of Strength 10 in the z-Direction

Dielectric constant ε	Dipole moment			Inside impending field		
	Calculated	Analytical	% Difference	Calculated	Analytical	% Difference
5	5074.7	5129.2	−1.06	−4.84	−4.90	−1.23
25	9008.5	8923.2	0.96	−8.51	−8.52	0.086
10^5	10968.0	10472.0	4.73	−10.18	−10.0	1.80

TABLE III

Comparison of Numerically Calculated and Analytical Results for the Dipole Moment (in the z-Direction) for a Dielectric Sphere of Radius 0.5 in an Electric Field Caused by a Point Charge of Value 2000 Located at a Distance 3 from the Center of the Sphere

Dielectric constant ε	Dipole moment		
	Calculated	Analytical	% Difference
5	−15.76	−15.87	−0.74
25	−24.86	−24.69	0.68
10^5	−28.98	−27.78	4.33

TABLE IV

Comparison of Numerically Calculated and Analytical Results for the Dipole Moment (in the z-Direction) for a Dielectric Sphere of Radius 0.5 and Dielectric Constant $\varepsilon = 5$ in an Electric Field Caused by a Point Charge of Value 2000 Located at Distance d from the Center of the Sphere, after Zero Total Charge Constraint Is Satisfied

Distance of charge	Dipole moment		
	Calculated	Analytical	% Difference
1.0	−139.29	−142.86	−2.50
0.7	−280.36	−291.55	−3.84

tric constant did reduce the difference between TPP and TNP by almost half, but not completely to zero.

With some effort, we found a rather simple approach to resolve the problem. Let us denote the sum of all solutions of the matrix equation (13) by S:

$$S = \sum_{i=1}^{B} \rho^i = \text{TPP} + \text{TNP}. \tag{28}$$

Physically, S should be zero. If it is not, we try to force it by distributing free charge $= -S$ on the dielectric sphere. The simplest way is to distribute it uniformly. Therefore, we add the free charge $\rho^0 = -S/B$ to each cell. The additional polarized charge of $\rho^{i'}$ at the ith volume element is given by matrix equation

$$A(\rho' + \rho^0) = -\rho^0, \tag{29}$$

where A is the matrix $a_{i,j}$. Rearranging the terms, one gets

$$A\rho' = -\rho^0(I - A). \tag{30}$$

Physically, the sum of this new polarized charge,

$$S' = \sum_{i=0}^{B} \rho^{i'}, \tag{31}$$

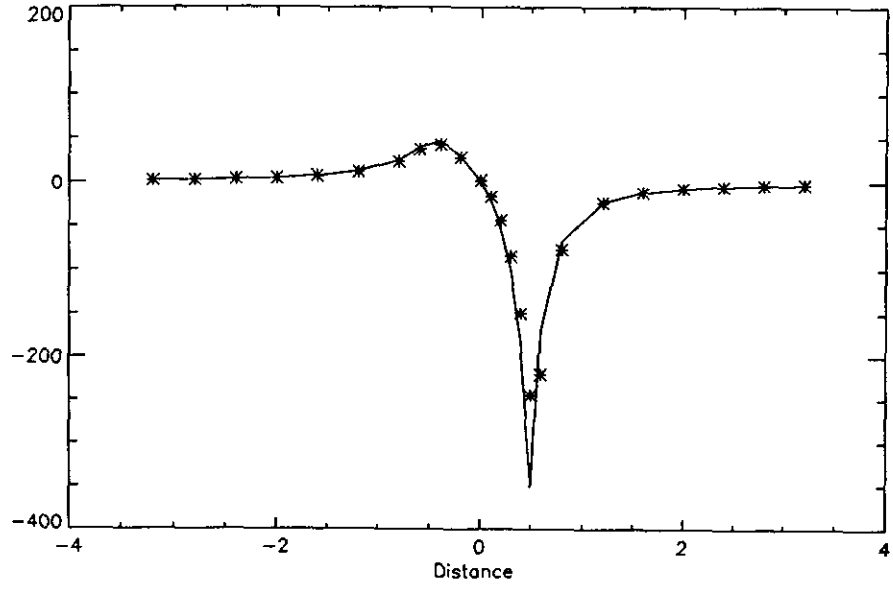

FIG. 4. Impending potential for a sphere of radius 0.5 with dielectric constant $\varepsilon = 5$ in the presence of a point charge of 2000 located at a distance 0.7 from its center. Solid line represents analytical results while * denotes the numerically calculated values.

should be zero. If not, we distribute $-S'$ free charge again on the sphere and determine the additional polarized charge. We need to continue this process until the sum of polarized charges approaches zero. By examining this process, fortunately we found that the ratio S'/S forms a geometrical series. Therefore, we do not have to follow the iterative process; instead the total charge needed in the volume element is

$$\rho^i = \frac{\rho^0 + \rho^{i'}}{1 - S'/S} \tag{32}$$

and the total free charge added is $-S$, which satisfies the zero total charge constraint.

In Table IV we give the values of dipole moment in the z-direction as calculated with the numerical method after implementing the above constraint for $d = 1.0$ and 0.7. Comparing them with the analytical values, one sees that they are quite good (but somewhat worse than those when the zero total charge constraint is not satisfied; see Table III). In Fig. 4 are given the impending potentials as calculated by numerical and analytical methods for $d = 0.7$. As we can see, the numerical value is within 5% of the analytical value.

4. CONCLUSION AND FUTURE WORK

In this series of two papers, we have presented two novel computationally faster approaches for solving the electrostatic problem for arbitrary inhomogeneous dielectric media with open boundary conditions. We tested them for three simple cases and they both seem to work quite well. The first method, the indirect boundary element method (IBEM), described in the first paper [1] is more accurate than the volume element method (VEM) described in this paper, but VEM is computationally faster; for the case of a dielectric sphere in a parallel field, for a $10 \times 10 \times 10$ grid, the CPU time for IBEM is 218.6 sec vs 14.5 sec for VEM. In the future, we plan to explore these methods further by applying them to complex problems and even solving problems other than electrostatic ones. It is conceivable that a hybrid of these methods will emerge as the optimal choice from the point of view of computational efficiency and accuracy.

REFERENCES

1. N. S. Goel, F. Gang, and Z. Ko, *J. Comput. Phys.* **118** (1995), 172–179.
2. S. Ratnajeevan and H. Hoole, *Computer-Aided Analysis and Design of Electromagnetic Devices* (Elsevier, New York, 1989).